Proceedings of the Korean Nuclear Society Autumn Meeting
Yongpyong, Korea, October 2002

Flow Characteristics of Sweepout and Entrainment in the Annular Downcomer

Sang H. Yoon, Kune Y. Suh*

Seoul National University
San 56-1 Sillim-Dong, Kwanak-Gu, Seoul, 151-742, Korea
*Phone: +82-2-880-8324, Fax: +82-2-889-2688, Email: kysuh@snu.ac.kr

Abstract

Sweepout from the water surface by gas (vapor or air) flow plays an important role in analyzing the mass and momentum transfer in the reactor downcomer of multidimensional geometry during a loss-of-coolant accident (LOCA) by decreasing the water level in the downcomer. The core water level will tend to decrease rapidly if a considerable amount of the entrained water stream and droplets bypasses through the break. The amount of entrained water is mostly determined by the interacting gas flow rate, the geometric condition, and the interfacial area between the gas and the water. The sweepout is observed to take place in three regions: the beginning of oscillation, the full wave and the wave peak (droplet separation). The beginning of oscillation normally occurs by the Helmholtz instability, which is defined in terms of the difference between the gas and the liquid velocities. The horizontal water surface is waved greatly before the gas flow reaches the critical point of droplet detachment. In the full-wave region, the droplets from the rough wave are swept into the gas flow and driven to the break. The water stream and droplets near the wave-peak region bypass through the break at extremely high velocities. In view of these observations we investigated the relation between the gas flow rate and the amount of bypass as a function of time. The test facility was constructed in a 1/10 linear scale-down model from the APR1400 (Advanced Power Reactor 1400MWe), which has four DVI (Direct Vessel Injection) lines, four cold legs, and two hot legs. The air was injected through the three intact cold legs and bypassed through the broken cold leg. The sweepout was visualized by using the acrylic test vessel. When the water level was located at the bottom of the break nozzle, the amount of bypass increased at the high Reynolds number of the gas. In the test the downcomer water level rapidly decreased for the initial one minute. Then, given the Reynolds number of the gas, the sweepout hardly occurred as the water level approached the critical point after ten minutes. So far, the experiment and the analysis for the sweepout have been limited to small annuli, flat plates and T-junctions, which yielded the two-dimensional flow field. The experimental results shed light on the flow mechanism and the semi-empirical relations for the sweepout phenomena, which has three-dimensional flow patterns in the large annulus as in the reactor case. The sweepout and entrainment are physically understood by visual inspection of flow in the downcomer. A physico-numerical model is being developed to

predict the multidimensional bypass flow rate resulting from the sweepout and entrainment in the downcomer.

1. Introduction

The sweepout from the water surface by the gas flow plays an important role in analyzing the multidimensional thermal hydraulics in the reactor downcomer during a loss-of-coolant accident (LOCA) by decreasing the water level in the downcomer [1]. As the gas flow increases, the water surface in the downcomer oscillates enough to cause liquid droplets to be torn off the wavy liquid-gas interface and entrained in the gas flow.

In the annular gap sweepout occurs by the Helmholtz instability [2] due to the two-phase velocity difference at the interface. In the multidimensional, curved, asymmetric surface as in the reactor downcomer, the impinged gas flow is slated to go through complex flow paths. So far, the sweepout studies have been limited to such rather simple geometries as small annuli [3], flat plates [4] and T-junctions, however.

The sweepout in the reactor downcomer may partly accelerate depletion of the core water inventory, which in turn may result in faster core uncovery to trigger premature core melting. The extent of water droplet entrainment is, however, limited since the sweepout takes place only until the critical void height is reached in the given geometry [5].

2. Sweepout Characteristics

Sweepout causes the core makeup water to be depleted by the droplet entrainment from the downcomer. The sweepout is generally affected by the geometry of the reactor piping system. For example, as shown in Fig. 1, the APR1400 (Advanced Power Reactor 1400MWe) has four cold legs, four DVI (Direct Vessel Injection) lines and two hot legs. In a cold-leg-break LOCA the horizontally injected gas flow sweeps away in the azimuthal direction through the downcomer.

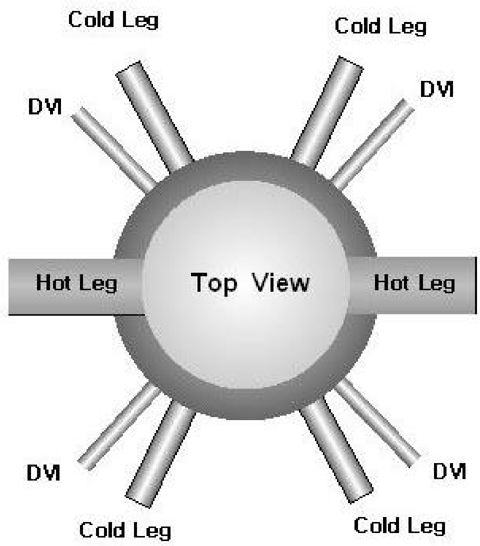

Fig.1 Reactor Vessel Top View

Generally, the gas flow is injected through three cold legs to the downcomer, except for the broken cold leg during a cold-leg-break LOCA. The sweepout can be described as the gas flow bypass over the free water surface when the core water level is as shown in Fig. 2. The sweepout is observed to take place in three distinct regions: the beginning of oscillation, the full wave and the wave peak (droplet separation).

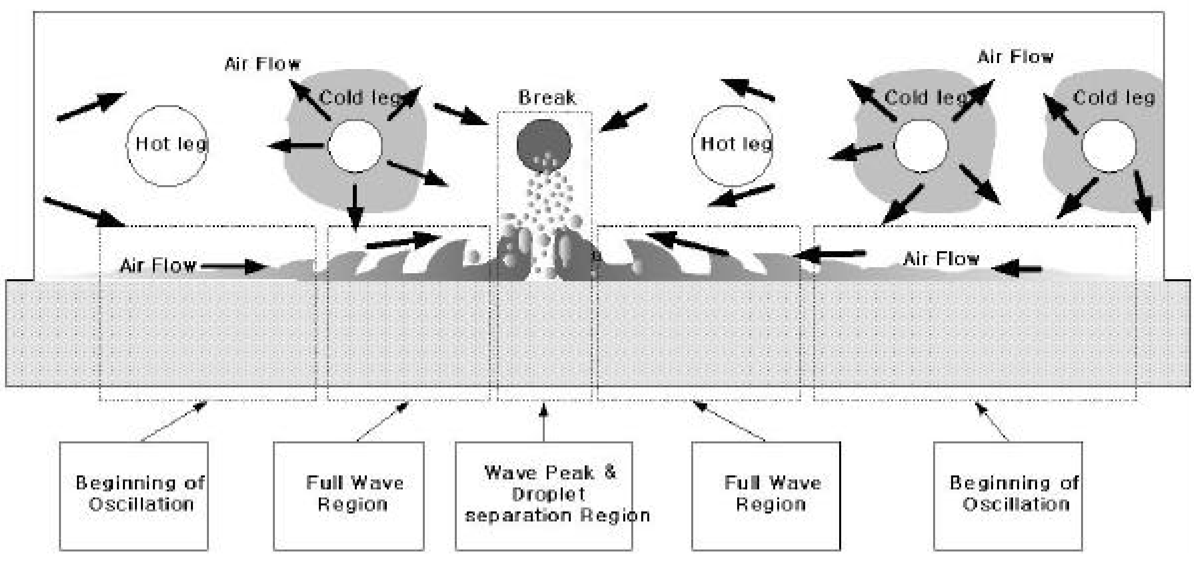

Fig. 2 Sketch of Multidimensional Sweepout

II.A. Beginning of Oscillation

The beginning-of-oscillation region is developed by the formation of roll waves due to the Helmholtz instability and asymmetry between the three cold legs and the break.

This region tends to be reduced as the injected gas flow rate increases. Figure 3 shows the growth of the roll wave by the asymmetric velocity distribution between the gas and the water free surface [6].

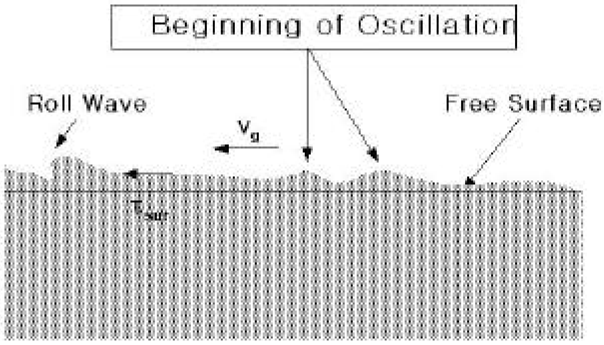

Fig. 3 Sketch of Beginning of Oscillation

II.B. Full Wave

As illustrated in Fig. 4 the full-wave region can be defined as the region where the wave heights greatly increase by the increase of the interfacial shear stress between the gas flow and the water free surface [7]. In this region the water level gets higher than in the beginning-of-oscillation region because of the pressure difference among the injection ports and the break. Then the droplet entrainment is initiated gradually [8].

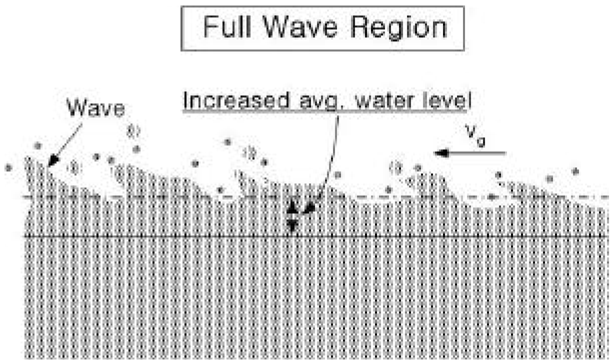

Fig. 4 Sketch of Full-Wave Region

II.C. Wave Peak (Droplet Separation)

The wave peak, or droplet separation, represents the region where a large amount of water is swept out through the break in the form of slugs and droplets off the swelled-up water level as depicted in Fig. 5. The entrainment is radically developed in the wave-peak region. In this region the internal and external vortices, or wave peaks, are formed by the collision of the asymmetric rough waves with the gas flow. These vortices accelerate the droplet entrainment in the wave-peak region and give rise to the droplet separation from the wave in the long run.

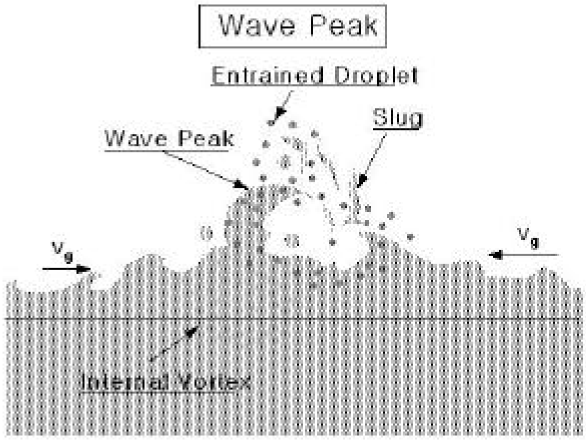

Fig. 5 Sketch of Beginning-of-Oscillation Region

3. Experimental Procedure

The present experiments were concerned with the multidimensional sweepout of water slugs or droplets off the free surface by the horizontally injected gas flow in the annular gap**.**

The test facilities were set up for the visualization of the sweepout and for the measurement of the critical void height in the transient state. Since the hydraulics in the downcomer is governed by the interaction between the gas flow and the free water surface, the experiments were focused on the liquid-gas flow distribution. Water and air were chosen as the working fluids as they were considered to yield more conservative result of sweepout than water and steam (which is condensable). In other words, as the steam condenses on the free surface, the relative velocity of the steam will tend to decrease. On the other hand, the air is noncondensable so that the critical void height should differ for the air or steam flow at the same velocity.

The tests were conducted pursuant to the following procedure.

To measure the transient critical void height from the bottom of the cold leg, the downcomer was filled with water up to the bottom of the cold legs. Then the changing water level was measured in the downcomer for varying air injection flow rates without external water supply.

To determine the air injection velocities in the tests use was made of the results from the Korea Atomic Energy Research Institute (KAERI) scaling analysis as summarized in Tables 1 and 2. The design values of the APR1400 were linearly scaled down to 1/10 as shown in Fig. 6. The average air injection velocities were 8.4, 13, 17.6, 21 and 23.3 m/s, respectively.

Table 1 Scaling Ratio for KAERI/SNU Tests

Parameter	Scaling Ratio			
	Modified Linear Scaling	KAERI	SNU	SNU/KAERI
Length Ratio, l_{oR}	l_R	1/7.071	1/10	0.7071
Area Ratio, a_{oR}	l_R^2	1/50	1/100	0.50
Volume Ratio, V_{oR}	l_R^3	1/353.55	1/1000	0.353
Time Ratio, t_{oR}	$l_R^{1/2}$	1/2.659	1/3.162	0.841
Velocity Ratio, v_{oR}	$l_R^{1/2}$	1/2.659	1/3.162	0.841
Flow Rate Ratio, $\dot{m}_{oR}$	$l_R^{5/2}$	1/132.95	1/316.22	0.42

Table 2 Gas Injection Velocity

	Average Gas Velocity at Each Intact Cold Leg(m/s)		
	Prototype(KNGR)	KAERI TEST	SNU TEST
1	13.295	5	4.205
2	26.59	10	8.41
3	39.885	15	12.6
4	53.18	20	16.82
5	66.475	25	21.0
6	79.77	30	25.23
7	85.088	32	26.9

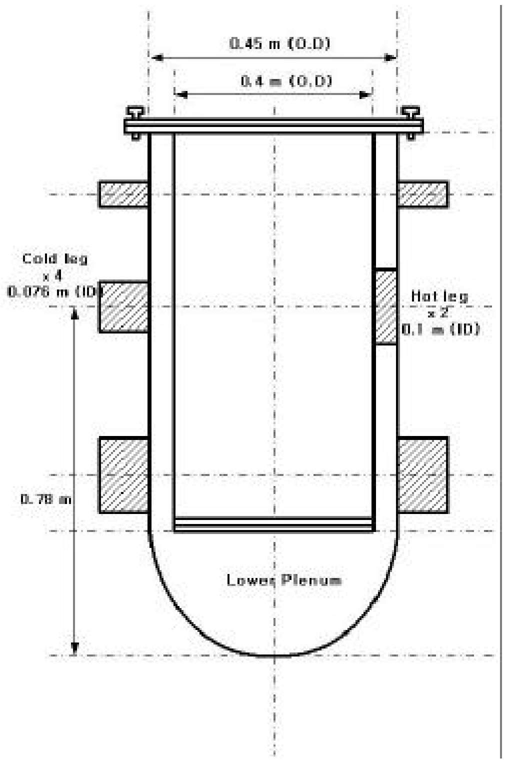

Fig. 6 Schematic of Simulating Acryl Vessel

The simulating acryl vessel was a 1/10 linearly scaled-down model so that the gap of the downcomer was determined as 0.025 m. The core thermal effect was not considered in the current tests. The transient water level was measured at the 2 cm decrease time interval.

4. Results and Discussion

Visualization and measurement of the sweepout clearly demonstrated the three flow regions. The tests showed the extended beginning-of-oscillation region at the low air velocity. The beginning-of-oscillation region was reduced at the high velocity. In the full-wave region the droplet entrainment rapidly began. The full-wave region expanded as the air velocity was increased. In the wave-peak, or droplet-separation, region the slugs and the droplets were formed by the circulation of the internal and external vortices.

As shown in Fig. 7, the water level reduction by the air velocity increase reached 90 % of the critical void height in about 60 s. Thus the amount of bypass was determined in about 60 s. After then, the water level reaches the critical void height during a long-term period (about 600 s).

Before about 60 s, the bypass by slug flow is more dominant and after about 60 s, the bypass by droplet flow is more dominant in the sweepout.

As the increase rate of the critical void height as shown in Fig. 8 is linearly proportional to that of the air injection velocity, one can predict the critical void height at any air velocities.

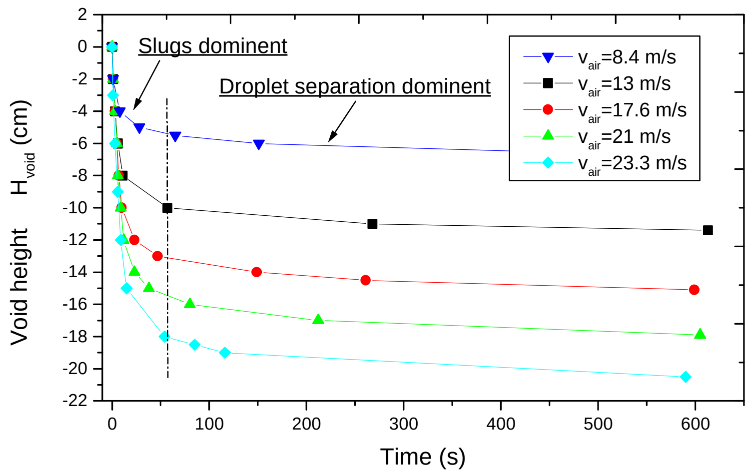

Fig. 7 Transient Void Height vs. Air Injection Velocity

Figure 9 demonstrates the sweepout at low air velocity. The water level difference between the beginning-of-oscillation and wave-peak (droplet-separation) regions is relatively small. The width between the beginning-of-oscillation and full-wave regions is very large.

Figure 10 shows the developing sweepout for the increased air velocity. The average downcomer water level is radically reduced. The width of the beginning-of-oscillation region is decreased. The full-wave region greatly increases by interference with the wave-peak, or droplet-separation, region. The internal vortex in the wave-peak region grows gradually.

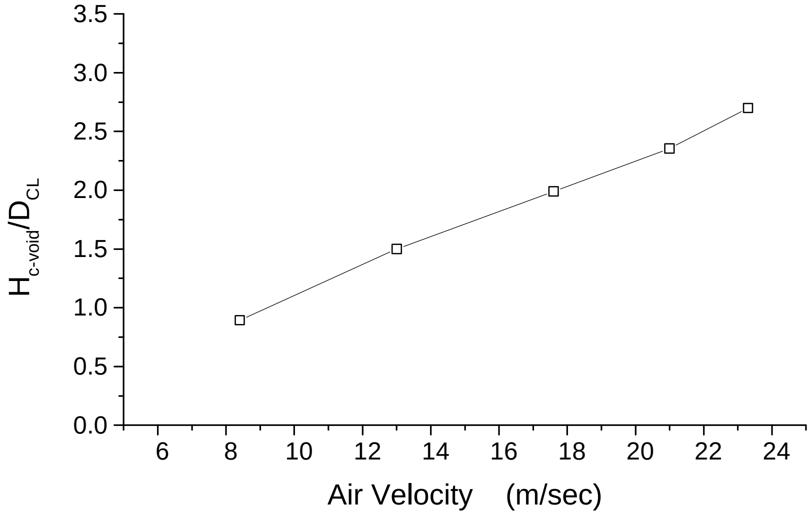

Fig. 8 Critical Void Height vs. Air Injection Velocity

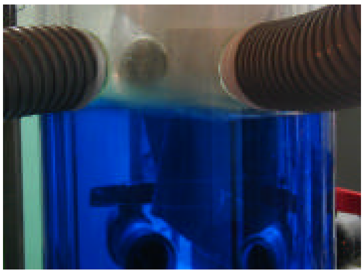

t = 40 s

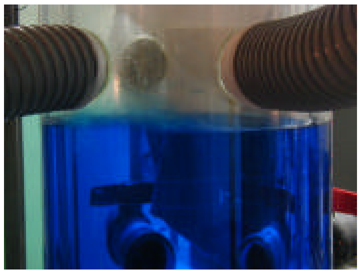

t = 100 s

Fig. 9 Sweepout Test at Air Velocity of 8.4 m/s

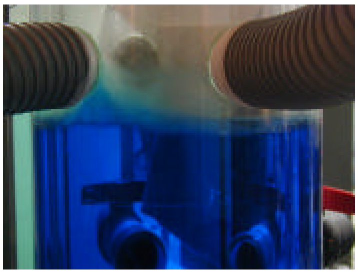

t = 40 s

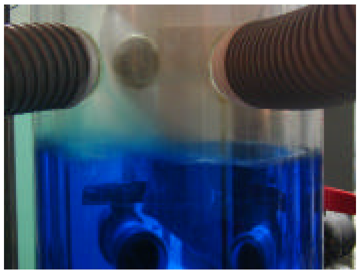

t = 100 s

Fig. 10 Sweepout Test at Air Velocity of 17 m/s

Figure 11 visualizes the fully developed sweepout at extremely high air velocity. The reduction rate of the water level is very large and the wave-peak (doplet-separation) region rapidly widens. The sweepout through the droplet entrainment occurs even at very low average water level and the internal and external vortices grow vigorously.

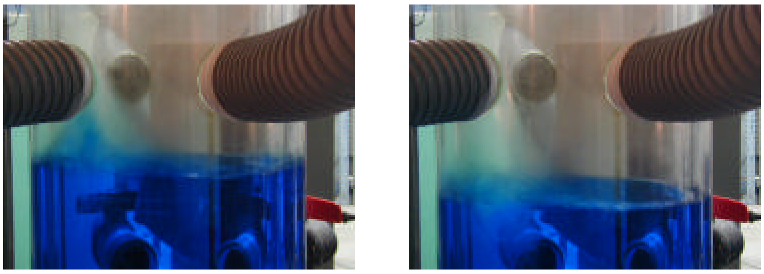

t = 40 s t = 100 s

Fig. 11 Sweepout Test at Air Velocity of 23.3 m/s

5. Conclusions

In the present empirical study the focus was placed on the multidimensional sweepout of water in the annular downcomer gap by the horizontally injected gas flow over the free surface.

The conclusions may be summarized as follows.

1. The bypass by the multidimensional sweepout can be classified into the following three regions due to the asymmetric geometry of the reactor piping system.
   - Beginning of oscillation
   - Full wave
   - Wave peak (droplet separation)

2. The bypass by the sweepout occurs in the form of slugs and droplets torn off the free surface of water.

3. In the transient the bypass by the slug flow is more dominant in the earlier phase, while the bypass by the droplet entrainment is more significant in the later phase.

4. The wave-peak (droplet-separation) region is formed by the asymmetric geometry and the interaction between the air flow and the water free surface in the annulus gap.

5. The bypass by the slugs and droplets results from the internal and external vortices in the wave-peak region.

The sweepout in the multidimensional curved surface in the reactor downcomer vividly demonstrates the three flow region characteristics. Work is in progress to predict the flow characteristics utilizing the analytical tool based on the experimental data. Results from this study will contribute to theorizing the basic sweepout phenomena for the reactor safety analysis.

Nomenclature

V_g = gas velocity
τ_{SUR} = shear stress at the free surface
V_{avg} = average air injection velocity
H_{void} = void height (in the middle of the test)
$H_{c\text{-}void}$ = critical void height (in the end of the test)
D_{CL} = diameter of the cold leg

References

1. M. Ishii, K. Mishima, “Droplet entrainment correlation in annular two-phase flow,” Int. J. Heat Mass Transfer, **Vol. 32,** No. 10, pp. 1427 (1989).
2. B. H. Kim, G. P. Peterson, “Analysis of the critical Weber number at the onset of liquid entrainment in the capillary-driven heat pipes,” Int. J. Heat Mass Transfer, **Vol. 38,** No. 8, pp. 1427 (1995).
3. A. Assad, C. Jan, M. Lopez de Bertodano, “Scaled entrainment measurements in ripple-annular flow in a small tube,” Nuclear Engineering and Design, **Vol. 184,** pp. 437-447 (1998)
4. M. R. Maier, H. M. Soliman, “Onsets of entrainment during dual discharge from a stratified two-phase region through horizontal branches with centerlines falling in an inclined plane : Part 2-Experiments on gas and liquid entrainment,” Int. J. Multiphase Flow, **Vol. 27,** pp. 1029-1049 (2001)
5. I. Kataoka, M. Ishii, A. Nakayama, “Entrainment and deposition rates of droplets in annular two-phase flow,” Int. J. Heat Mass Transfer, **Vol. 43,** pp. 1573-1589 (2000)
6. J. W. Miles, “On the generation of surface waves by turbulent shear flows,” J. Fluid Mechanics, **Vol. 7,** pp. 469-478 (1959).
7. M. J. Lighthill, “Physical interpretation of the mathematical theory of wave generation by wind,” J. Fluid Mechanics, **Vol. 14,** pp. 385-398 (1962).
8. M. L. Banner, W. K. Melville, “On the separation of air flow over water waves,” J. Fluid Mechanics, **Vol. 77,** pp. 825-842 (1976).